

Frascati Physics Series Vol. XXIV (2002), pp. 363-380  
INTERNATIONAL SCHOOL OF SPACE SCIENCE - 2001 Course on  
ASTROPARTICLE AND GAMMA-RAY PHYSICS IN SPACE, L'Aquila (Italy), 30/8 - 7/9, 2001

## **GAMMA RAY ASTROPARTICLE PHYSICS WITH GLAST**

Aldo Morselli

*Dept. of Physics, Univ. of Roma "Tor Vergata" and INFN Roma 2, Italy*

### **ABSTRACT**

The energy domain between 10 MeV and hundreds of GeV is an essential one for the multifrequency study of extreme astrophysical sources. The understanding of spectra of detected gamma rays is necessary for developing models for acceleration, emission, absorption and propagation of very high energy particles at their sources and in space. After the end of EGRET on board the Compton Gamma Ray Observatory this energy region is not covered by any other experiment, at least up to 50 GeV where ground Cerenkov telescopes are beginning to take data. Here we will review the status of the space experiment GLAST that will fill this energy region from March 2006 with particular emphasis at the connection with all the other ground and space planned experiments and at the contribution of GLAST to particle physics.

## 1 GLAST

The techniques for the detection of gamma-rays in the pair production regime energy range are very different from the X-ray detection ones. For X-rays detection focusing is possible and this permits large effective area, excellent energy resolution, very low background. For gamma-rays no focusing is possible and this means limited effective area, moderate energy resolution, high background but a wide field of view (see figure 1). This possibility to have a wide field of view is enhanced now, in respect to EGRET, with the use of silicon detectors, that allow a further increase of the ratio between height and width (see fig.2), essentially for two reasons: a) an increase of the position resolution that allow a decrease of the distance between the planes of the tracker without affect the angular resolution, b) the possibility to use the silicon detectors themselves for the trigger of an events, with the elimination of the Time of Flight system, that require some height.

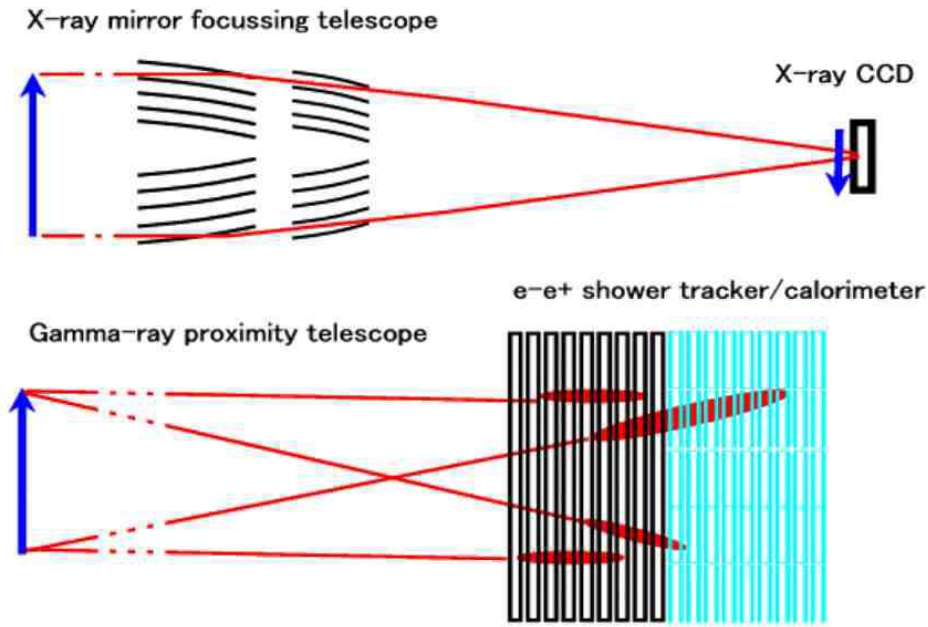


Figure 1: *Detector Technology: X-ray versus Gamma-ray.*

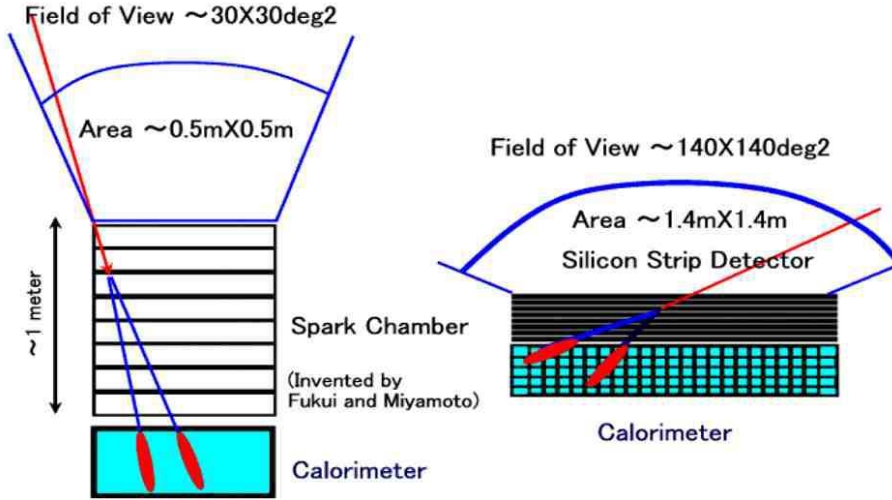


Figure 2: *EGRET*(Spark Chamber) versus *GLAST* (Silicon Strip Detector).

The Gamma-ray Large Area Space Telescope (GLAST) <sup>1)</sup>, has been selected by NASA as a mission involving an international collaboration of particle physics and astrophysics communities from the United States, Italy, Japan, France and Germany for a launch in the first half of 2006. The main scientific objects are the study of all gamma ray sources such as blazars, gamma-ray bursts, supernova remnants, pulsars, diffuse radiation, and unidentified high-energy sources. Many years of refinement has led to the configuration of the apparatus shown in figure 3, where one can see the 4x4 array of identical towers each formed by: • Si-strip Tracker Detectors and converters arranged in 18 XY tracking planes for the measurement of the photon direction. • Segmented array of CsI(Tl) crystals for the measurement the photon energy. • Segmented Anticoincidence Detector (ACD). The main characteristics are an energy range between 20 MeV and 300 GeV, a field of view of  $\sim 3$  sr, an energy resolution of  $\sim 5\%$  at 1 GeV, a point source sensitivity of  $2 \times 10^{-9}$  (ph cm $^{-2}$  s $^{-1}$ ) at 0.1 GeV, an event deadtime of 20  $\mu$ s and a peak effective area of 10000 cm $^2$ , for a required power of 600 W and a payload weight of 3000 Kg.

The list of the people and the Institution involved in the collaboration together with the on-line status of the project is available at <http://www-glast.stanford.edu>. A description of the apparatus can be found in <sup>2)</sup>.

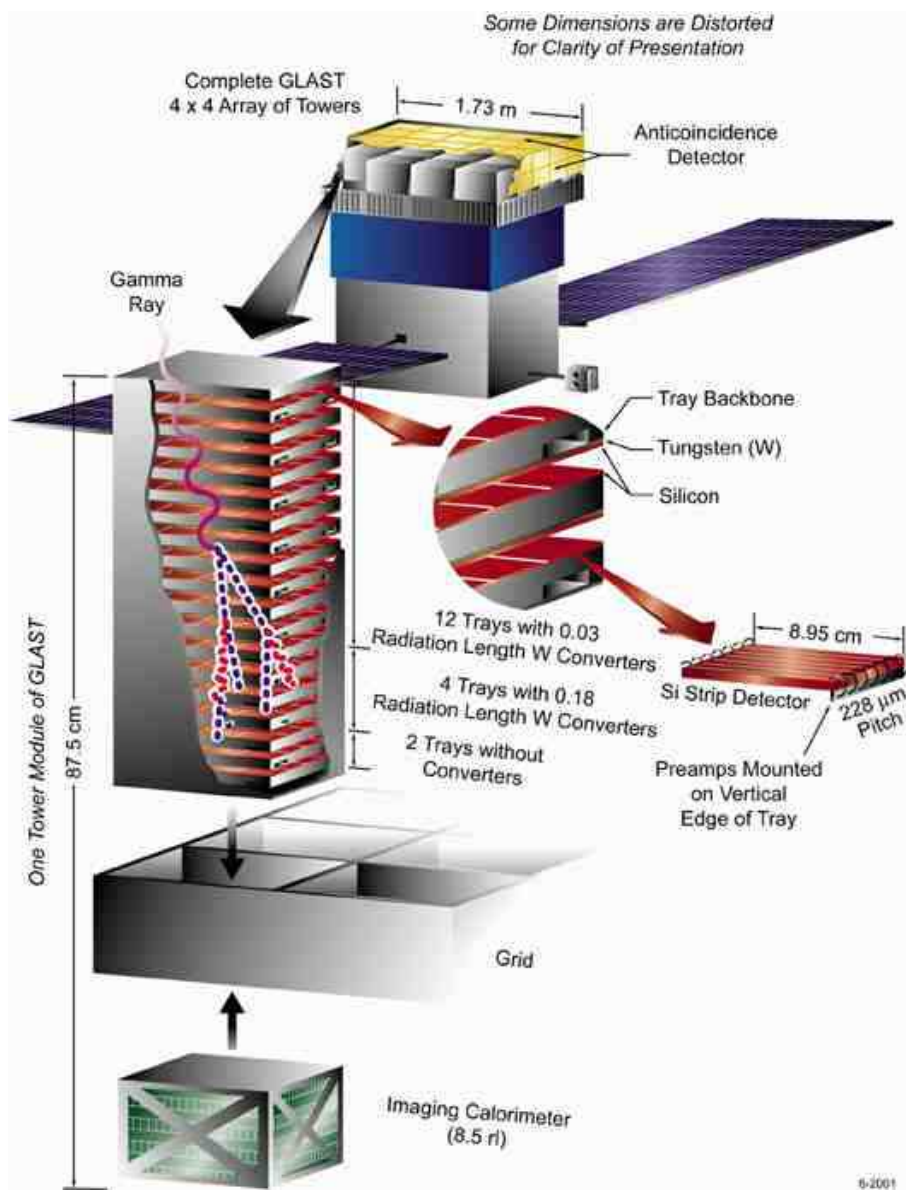


Figure 3: *The GLAST instrument, exploded to show the detector layers in a tower, the stacking of the CsI logs in the calorimeter, and the integration of the subsystems.*

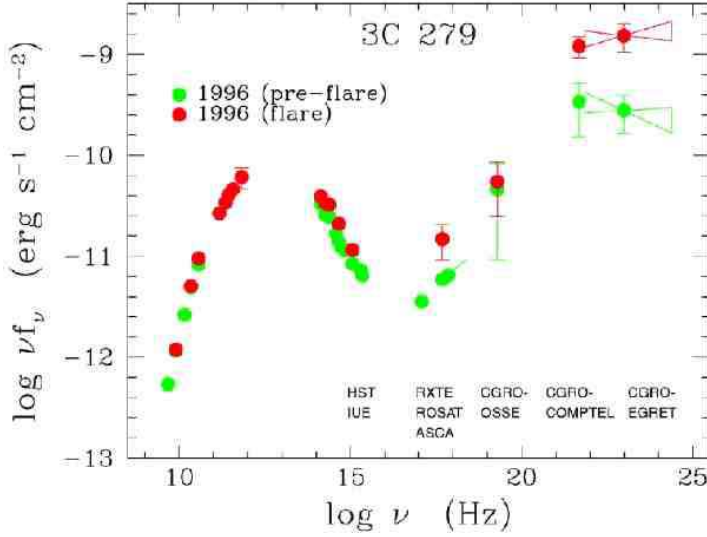


Figure 4: *Spectral energy distributions of the quasar 3C 279 during flaring state (in red) and non flaring state (in green).*

### 1.1 Active Galactic Nuclei

Before EGRET, 3C 273 was the only active galactic nucleus (AGN) known to emit high-energy gamma rays. Now we know that there is an entire class of active galaxies that probably represent the largest class of high energy gamma-ray emitters: the blazars. Blazars are flat radio spectrum, active galactic nuclei, or AGN, whose members include BL Lac objects and highly polarized and optically violently variable quasars that often emits more in gamma-ray than in any other frequencies (see figure 4). For a review on AGNs see reference <sup>3</sup>). GLAST will dramatically extend the number of observed AGNs, as well as the energy range over which they can be observed. Indeed, GLAST might be called the "Hubble Telescope" of gamma-ray astronomy as it will be able to observe AGN sources to  $z \sim 4$  and beyond, if such objects actually existed at such early times in the universe. Figure 5 shows the so called Log N versus Log S distribution, where N is the number of sources and S is source flux for  $E_\gamma > 100$  MeV, for AGN. The curve is extrapolated from EGRET data and an AGN model of the diffuse gamma-ray background based on the assumption that

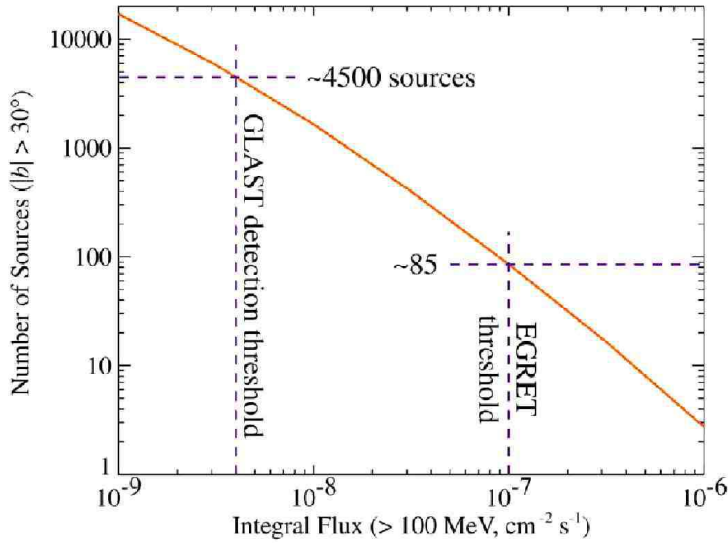


Figure 5: Estimate of the number of AGNs that GLAST will detect at high latitude in a 2 year sky survey compared to EGRET's approximate detection limit <sup>4)</sup>.

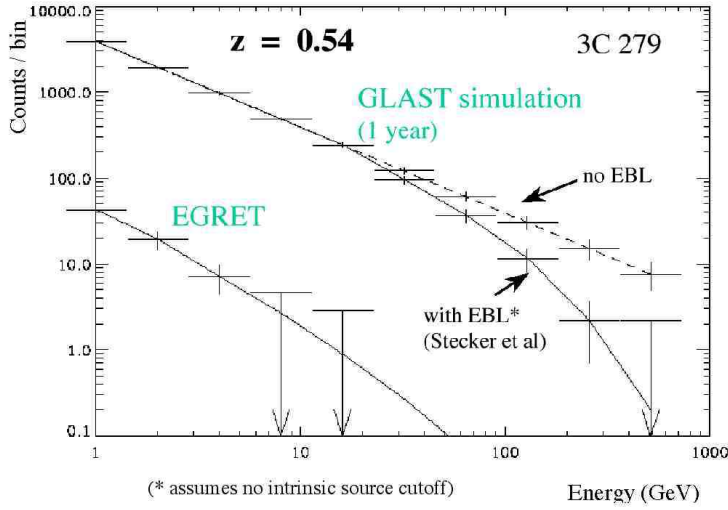


Figure 6: Number of photons detected by EGRET from 3C279 and the number expected with GLAST in the case of extragalactic background light attenuation and without attenuation <sup>5)</sup>.

AGN sources follow a luminosity function similar to flat spectrum radio quasars. Extrapolation from EGRET AGN detections projects that about 5,000 AGN sources will be detected in a 2 year cumulative scanning mode observation by GLAST, as compared to the 85 that have been observed by EGRET in a similar time interval. This large number of AGN's covering a redshift range from  $z \sim 0.03$  up to  $z \sim 4$  will allow to disentangle an intrinsic cutoff effect, i.e., intrinsic to the source, from a cut-off derived from the interaction with the extra galactic background light, or EBL. Only by observing many examples of AGN, and over a wide range of redshifts, one can hope to untangle these two possible sources of cutoff. In figure 6 is shown the number of photons detected by EGRET from 3C279 and the number expected with GLAST in the case of extragalactic background light attenuation and without attenuation. Determination of the EBL can provide unique information on the formation of galaxies at early epochs, and will test models for structure formation in the Universe.

## 1.2 Gamma-ray burst

Gamma-ray bursts (GRBs) are intermittently the most intense and most distant known sources of high-energy gamma rays; at GeV energies, the brightest GRBs are 1000-10,000 times brighter than the brightest AGN. The unparalleled luminosities and cosmic distances of GRBs, combined with their extremely fast temporal variability, make GRBs an extremely powerful tool for probing fundamental physical processes and cosmic history.

GLAST, in concert with the Gamma-ray Burst Monitor, will measure the energy spectra of GRBs from a few keV to hundreds of GeV during the short time after onset when the vast majority of the energy is released. GLAST will also promptly alert other observers, thus allowing the observations of GLAST to be placed in the context of multiwavelength afterglow observations, which are the focus of HETE-2 and the upcoming Swift missions. The additional information available from GLAST's spectral variability observations will be key to understanding the central engine.

Figure 7 illustrates a very intense, short GRB. The true EGRET time profile is very uncertain because the  $\sim$  two hundred milliseconds EGRET dead time per photon is comparable to GRB pulse widths; hence, many more photons may have been incident on EGRET during the extremely intense initial pulse. The GLAST dead time will be  $\sim$  10,000 times smaller, thus allowing a precise

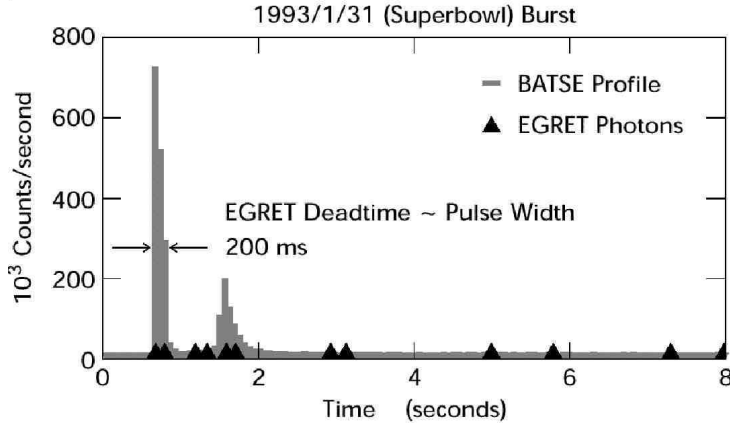


Figure 7: *EGRET* and *BATSE* light curves of the Superbowl burst, GRB930131. The burst consisted of an extremely intense spike, followed by low-level emission for several seconds. The true temporal development at energies  $>100$  MeV is uncertain since *EGRET* dead time is comparable to GRB pulse widths.

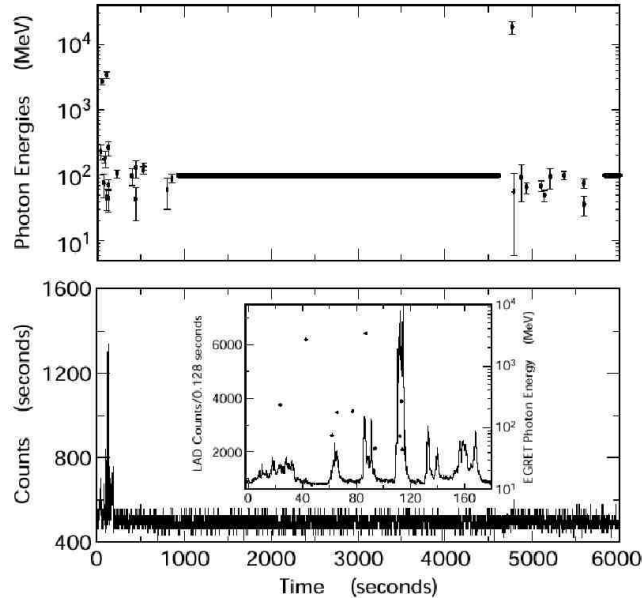


Figure 8: *EGRET* and *BATSE* light curves of GRB940217. Burst cessation at *BATSE* energies occurs at 160 s. Extended emission at *EGRET* energies persist beyond an intervening earth occultation, up to 5000 seconds after the *BATSE* event.



measurement of the gamma-ray flux during the peak.

This characteristic together with its larger field of view and larger effective area, should permit to detect virtually all GRBs in its field of view reaching the "the edge" of the GRB distribution, as does BATSE. Figure 8 shows another intense burst with very different temporal character which occurred in EGRET's field of view on 1994 Feb 17. At BATSE energies (25 - 1000 keV), this event persisted for  $\sim 160$  s; however, at EGRET energies, it apparently continued at a relatively high flux level past an Earth occultation, for at least 5000 s, to deliver a delayed  $\sim 18$  GeV photon. GLAST, with negligible self veto, will have good efficiency above 10 GeV and it will be able to localize GRBs with sufficiently high accuracy to enable rapid searches at all longer wavelengths. About half of the 200 bursts per year detected by GLAST will be localized to better than 10 arc minute radius, an easily imaged field for large-aperture optical telescopes.

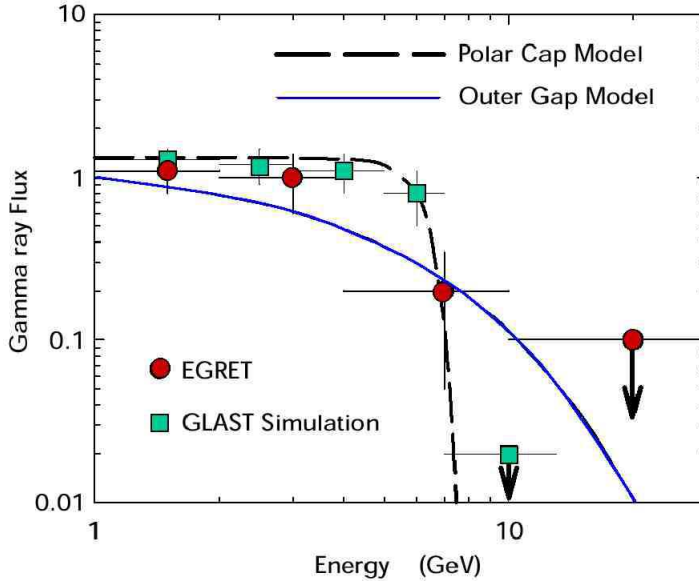


Figure 9: *Modeled high-energy pulsar spectrum, showing the improvement in resolution between EGRET and GLAST. The polar cap model predicts a sharp high-energy cutoff, while the outer gap model predicts a more gradual cutoff. Unlike EGRET, GLAST will be able to distinguish the true shape of the spectrum (assumed to be that of the polar cap model in this simulation).*

### 1.3 Pulsars

GLAST will discover many gamma-ray pulsars, potentially 50 or more, and will provide definitive spectral measurements that will distinguish between the two primary models proposed to explain particle acceleration and gamma-ray generation: the outer gap <sup>6)</sup> and polar cap models <sup>7)</sup> ( see figure 9). From observations made with gamma ray experiments through the EGRET era, seven gamma-ray pulsars are known. GLAST will detect more than 100 pulsars and will be able to directly search for periodicities in all EGRET unidentified sources. Because the gamma-ray beams of pulsars are apparently broader than their radio beams, many radio-quiet, Geminga-like pulsars likely remain to be discovered.

### 1.4 Search for supersymmetric dark matter

GLAST is particularly interesting for the supersymmetric particle search because, if neutralinos make up the dark matter of our galaxy, they would have non-relativistic velocities, hence the neutralino annihilation into the gamma gamma and gamma Z final states can give rise to gamma rays with unique energies  $E_\gamma = M_\chi$  and  $E'_\gamma = M_\chi (1 - m_z^2/4M_\chi^2)$ .

In figure 10 is shown how strong can be the signal <sup>8)</sup> in the case of a cuspy dark matter halo profiles distribution <sup>9)</sup>.

Figure 11 shows the GLAST capability to probe the supersymmetric dark matter hypothesis <sup>8)</sup>. The various zone sample the MSSM with different values of the parameters space for three classes of neutralinos. The previous galaxy dark matter halo profile <sup>9)</sup> that gives the maximal flux has been assumed. The solid line shows the number of events needed to obtain a  $5\sigma$  detection over the galactic diffuse  $\gamma$ -ray background as estimated from EGRET data. As the figures show, a significant portion of the MSSM phase space is explored, particularly for the higgsino-like neutralino case.

This effort will be complementary to a similar search for neutralinos looking with cosmic-ray experiments like the next space experiment PAMELA <sup>10)</sup> at the distortion of the secondary positron fraction and secondary antiproton flux induced by a signal from a heavy neutralino.

In figure 12 (on the left) there are the experimental data <sup>11)</sup> for the positron fraction together with the distortion of the secondary positron fraction

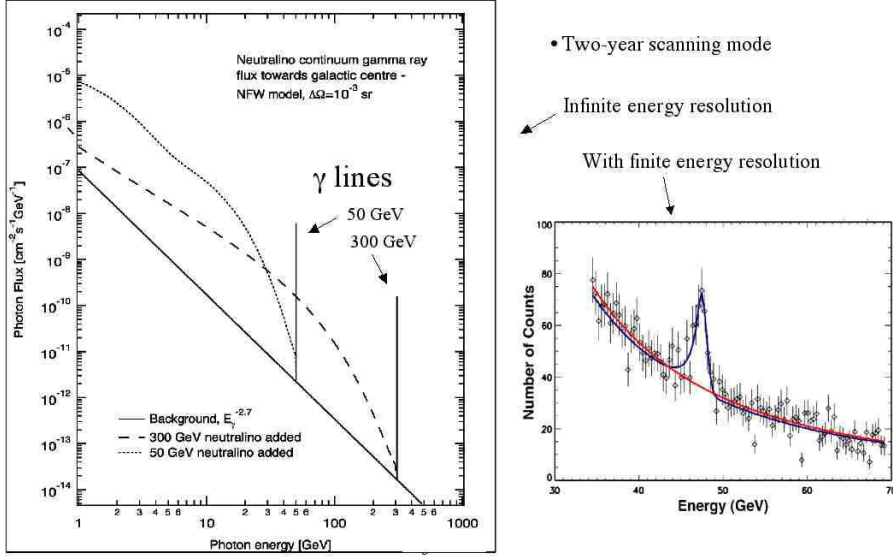


Figure 10: Total photon spectrum from the galactic center from  $\chi\chi$  annihilation (on the left), and number of photons expected in GLAST for  $\chi\chi \rightarrow \gamma\gamma$  from a 1-sr cone near the galactic center with a 1.5 % energy resolution (on the right)

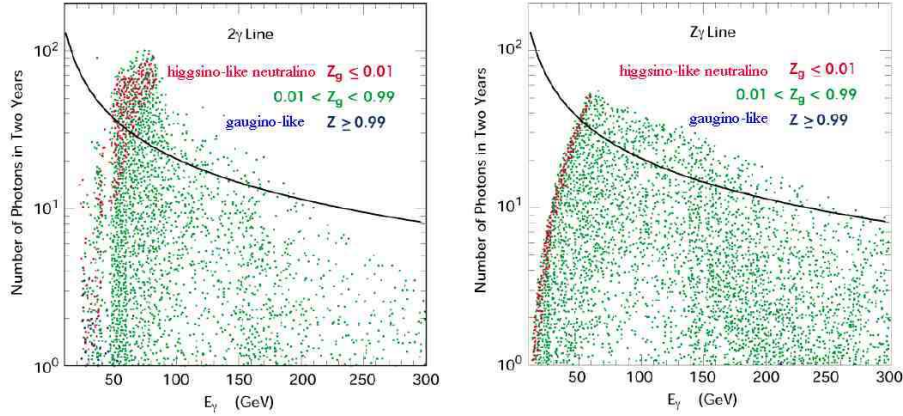


Figure 11: Number of photons expected in GLAST for  $\chi\chi \rightarrow \gamma\gamma$  from a 1-sr cone near the galactic center as a function of the possible neutralino mass. The solid line shows the number of events needed to obtain a five sigma signal detection over the galactic diffuse gamma-ray background as estimated by EGRET data.

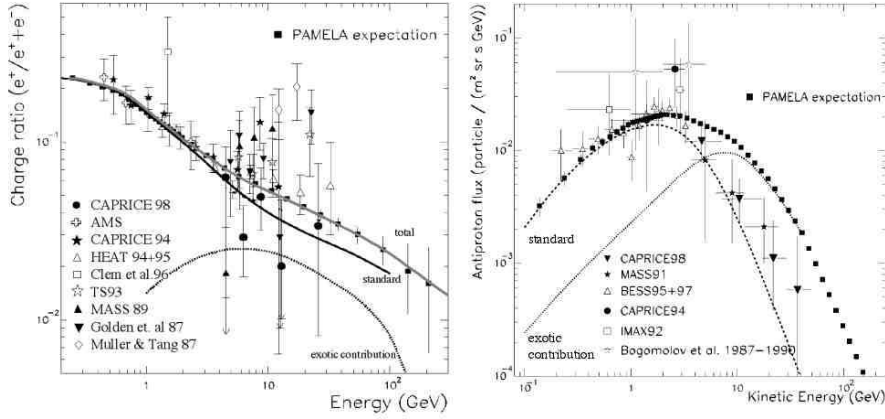


Figure 12: *Distortion of the secondary positron fraction (on the left) and secondary antiproton flux (on the right) induced by a signal from a heavy neutralino. The PAMELA expectation in the case of exotic contributions are shown by black squares*

(solid line) due to one possible contribution from neutralino annihilation (dotted line, from <sup>12</sup>). The expected data from the experiment PAMELA in the annihilation scenario for one year of operation are shown by black squares <sup>13</sup>).

In the same figure (on the right) there are the experimental data for the antiproton flux <sup>14</sup>) together with the distortion on the antiproton flux (dashed line) due to one possible contribution from neutralino annihilation (dotted line, from <sup>15</sup>). The antiproton data that PAMELA would obtain in a single year of observation for one of the Higgsino annihilation models are shown by black squares.

## 2 Conclusion

The gamma-ray space experiment GLAST is under construction. Its time of operation and energy range is shown together with the other space X-ray satellite and gamma-ray experiments in figure 13. Note that it will cover an interval not covered by any other experiments. Note also the number of other experiments in other frequencies that will allow extensive multifrequency studies.

## Energy versus time for X and Gamma ray detectors

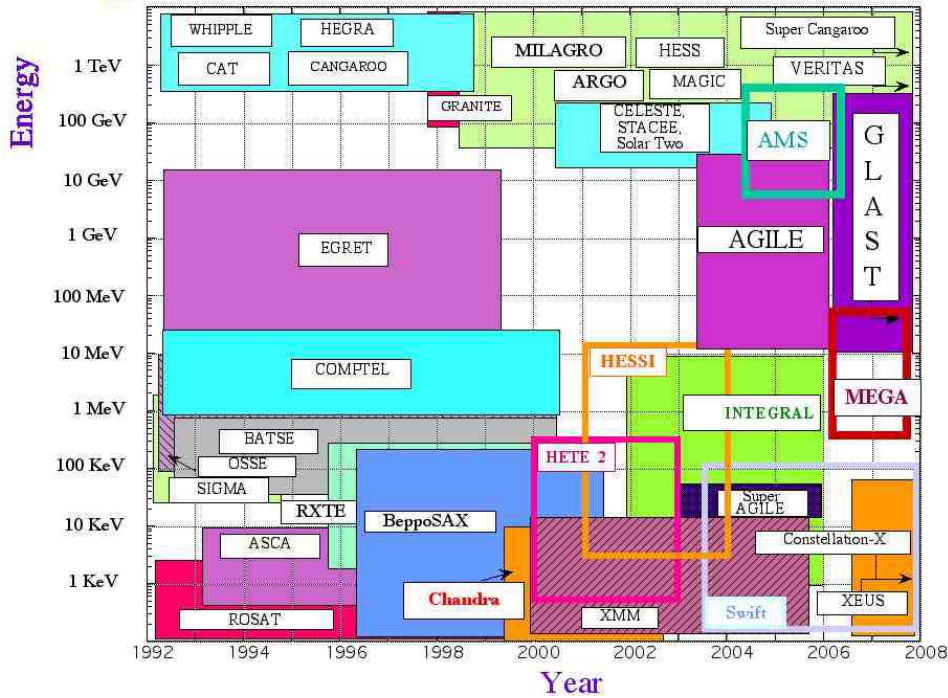


Figure 13: *Timeline schedule versus the energy range covered by present and future detectors in X and gamma-ray astrophysics.*

In the last decade, ground-based instruments have made great progress, both in technical and scientific terms. High-energy gamma rays can be observed from the ground by experiments that detect the air showers produced in the upper atmosphere. Air shower arrays directly detect the particles (electrons, muons, and photons) in air showers, and atmospheric Cerenkov telescopes detect the Cerenkov radiation created in the atmosphere and beamed to the ground. Detectors based on the atmospheric Cerenkov technique consist of one or more mirrors that concentrate the Cerenkov photons onto fast optical detectors. Photomultiplier tubes (PMTs) placed in the focal plane are generally used to detect the Cerenkov photons. Two problems in using atmospheric Cerenkov telescopes (ACT) are the night-sky background and the large isotropic background from cosmic-ray showers.

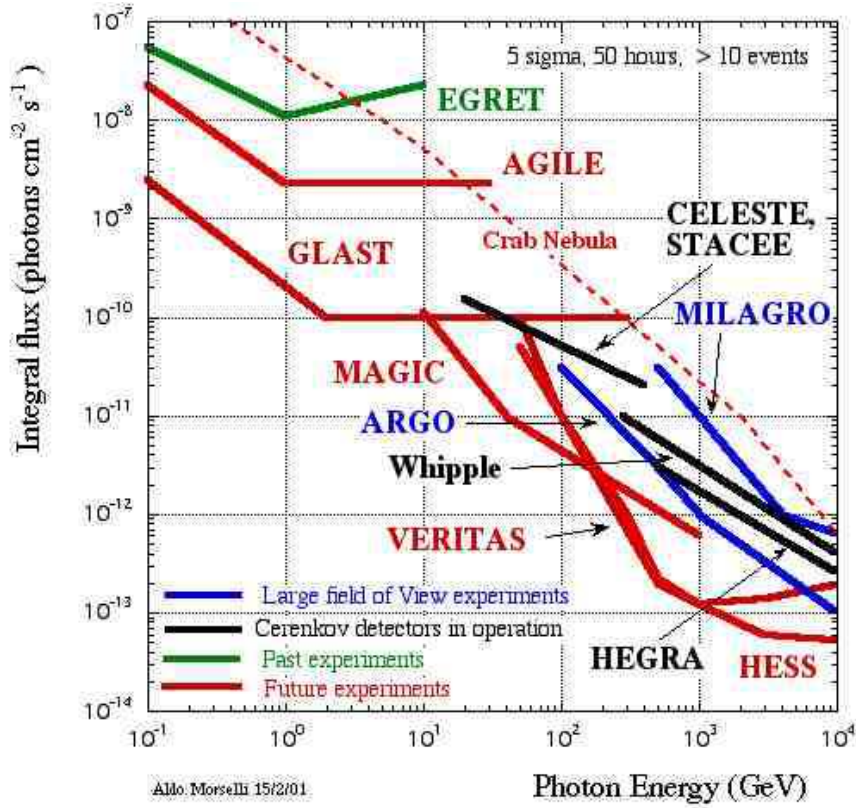


Figure 14: *Sensitivity of present and future detectors in the gamma-ray astrophysics.*

The energy threshold of an atmospheric Cherenkov telescope is determined by the number of Cherenkov photons needed to observe a signal above the level of the night-sky background. For individual point sources, ground-based instruments have unparalleled sensitivity at very high energies (above 50-250 GeV). For many objects, full multi-wave-length coverage over as wide an energy range as possible will be needed to understand the acceleration and gamma-ray production mechanisms. On the technical side, atmospheric Cherenkov telescopes have demonstrated that a high degree of gamma/hadron discrimination and a source pointing accuracy of 10-30 arc minutes (depending

on the source strength) can be achieved based on the detected Cherenkov image. Also the energy threshold is lowering remarkably (for a review, see <sup>16)</sup>). In figure 14 the GLAST sensitivity compared with the others present and future detectors in the gamma-ray astrophysics range is shown. The predicted sensitivity of a number of operational and proposed Ground based Cherenkov telescopes, CELESTE, STACEE, VERITAS, Whipple is for a 50 hour exposure on a single source. EGRET, GLAST, MILAGRO, ARGO and AGILE sensitivity is shown for one year of all sky survey. The diffuse background assumed is  $2 \cdot 10^{-5} \text{ photons cm}^{-2} \text{ s}^{-1} \text{ sr}^{-1} (100 \text{ MeV}/E)^{1.1}$ , typical of the background seen by EGRET at high galactic latitudes. The source differential photon number spectrum is assumed to have a power law index of -2, typical of many of the sources observed by EGRET and the sensitivity is based on the requirement that the number of source photons detected is at least 5 sigma above the background. Note that on ground only MILAGRO and ARGO will observe more than one source simultaneously. The Home Pages of the various instruments are at <http://www-hfm.mpi-hd.mpg.de/CosmicRay/CosmicRaySites.html>. A wide variety of experiments provide interesting probes for the search of supersymmetric dark matter. Indirect dark matter searches and traditional particle searches are highly complementary. In the next five years, an array of experiments will be sensitive to the various potential neutralino annihilation products. These include under-ice and underwater neutrino telescopes, atmospheric Cerenkov telescopes and the already described space detectors GLAST and PAMELA together with AMS. In many cases, these experiments will improve current sensitivities by several orders of magnitude. Direct dark matter probes share features with both traditional and indirect searches, and have sensitivity in both regions. In the cosmologically preferred regions of parameter space with  $0.1 < \Omega_\chi h^2 < 0.3$ , all models with charginos or sleptons lighter than 300 GeV will produce observable signals in at least one experiment. An example <sup>17)</sup> is shown in figure 15 in the framework of minimal supergravity, which is fully specified by the five parameters (four continuous, one binary)  $m_0, M_{1/2}, A_0, \tan \beta, \text{sgn}(\mu)$ . Here,  $m_0$ ,  $M_{1/2}$ , and  $A_0$  are the universal scalar mass, gaugino mass, and trilinear scalar coupling <sup>17)</sup>. The figure shows the limits that can be obtained in the  $m_0, M_{1/2}$  plane for  $\tan \beta = 10$ ,  $A_0 = 0$ ,  $\mu > 0$ . Higher values ( $\sim 50$ ) of  $\tan \beta$  requires significant fine-tuning of the electroweak scale. The limit from gamma-ray assumes a moderate halo profile.



## Estimated reaches before LHC

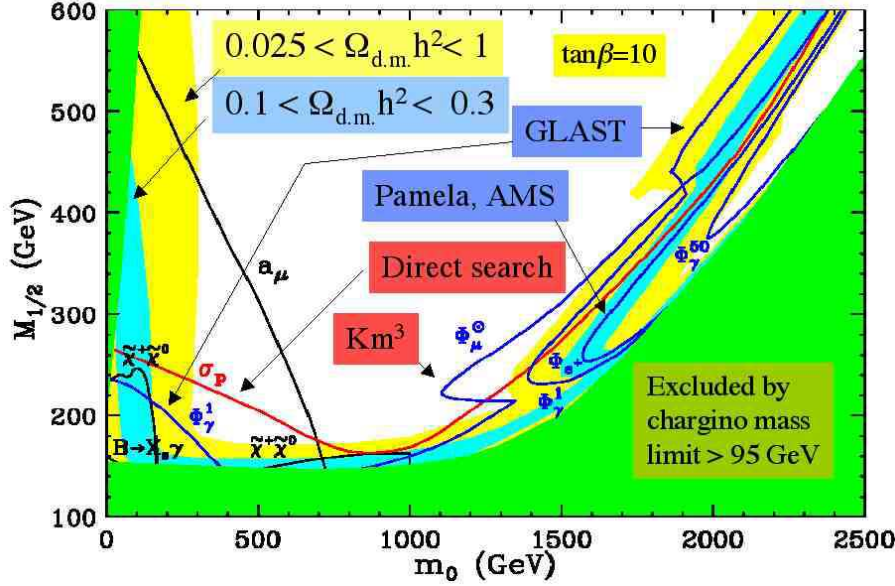


Figure 15: *Example of estimated reaches of various searches before the LHC begins operation. Note the complementarity between the different techniques. For moderate values of  $\tan\beta$  all the cosmological interesting region will be covered (see text for details).*

The  $a_\mu$  curve refers to the expected region that will be probed before 2006 by the measurements of the muon magnetic dipole moment <sup>18)</sup>. The curve  $B \rightarrow X_s \gamma$  refers to the improvement expected for the same date from BaBar, BELLE and B factories in respect to the CLEO and ALEPH results <sup>19)</sup>. The curve  $\Phi_\mu^\odot$  refers to the indirect DM search with underwater  $\nu$  experiments like AMANDA, NESTOR and ANTARES <sup>20)</sup> and the curve  $\sigma_p$  refers to the direct DM search with underground experiments like DAMA, CDMS, CRESST and GENIUS <sup>21)</sup>

We conclude with one last remark, the angular resolution and energy resolution achievable in gamma ray astrophysics is still lower to what is desirable and achievable in other band; so a long term plan like the one sketch in figure 16



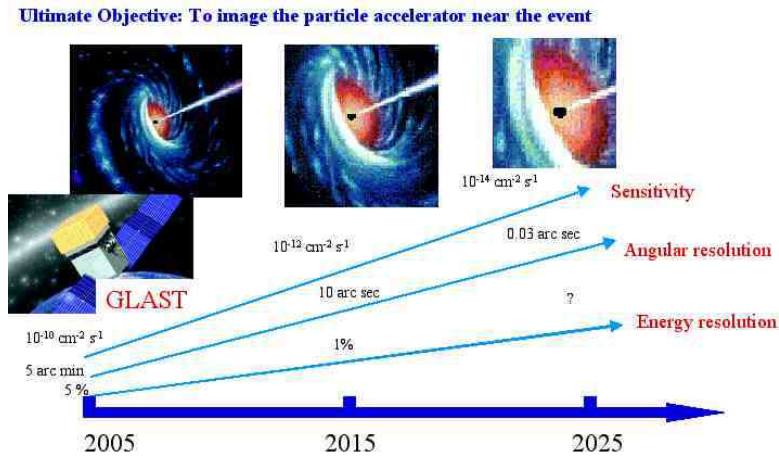


Figure 16: *Gamma-Ray Astronomy Long Term Plan*

is needed and can bring spectacular results.

### 3 Acknowledgments

I wish to thanks all the participants to the school. Everybody (both professors and students) contributes so much to discussions and debates to make the time spent in L'Aquila really very interesting.

### References

1. W. Atwood *et al.*, 1994, NIM, **A342**, 302. Proposal for the Gamma-ray Large Area Space Telescope, SLAC-R-522 (1998). B. Dingus *et al.*, 25th ICRC, OG 10.2.17, **5**, p.69, Durban. A. Morselli, Very High Energy Phenomena in the Universe, Ed. Frontiers (1997) 123.
2. R. Bellazzini, Frascati Physics Series Vol.XXIV, 353, (2002), <http://www.roma2.infn.it/inf/aldo/ISSS01.html>.
3. A. Celotti, Frascati Physics Series Vol.XXIV, 391, (2002), <http://www.roma2.infn.it/inf/aldo/ISSS01.html>.
4. F.W. Stecker, O. C. De Jager & M. H. Salamon, *Astrophys. J.* **L49**, 390(1992).

5. figure based on F.W. Stecker et al. 1992, *Astrophys. J. Lett.* **3990**, L49.
6. R. Romani, 1996, *Astrophys. J.* **470**, 469.
7. J. Daugherty and A. Harding, 1996, *Astrophys. J.* **458**, 278.
8. L. Bergström *et al.*, *Astropart. Phys.* **9**, 137, (1998).
9. J. Navarro *et al.*, *Astrophys. J.* **462**, 563(1996).
10. P. Spillantini *et al.*, 24th ICRC Roma, OG 10.3.7, 591, (1995).  
P. Spillantini, Frascati Physics Series Vol. XXIV, 249, (2002),  
<http://www.roma2.infn.it/inf/aldo/ISSS01.html>.
11. M. Boezio *et al.*, 2000, *ApJ*, **532**, 653 and references therein.
12. E. Baltz and J. Edsjö 1999 *Phys. Rev. D* **59**, 023511.
13. P. Picozza and A. Morselli, The Ninth Marcel Grossmann Meeting, World Scientific (2001) [astro-ph/0103117] and references therein.
14. D. Bergström *et al.*, 2000 *ApJ Letters*, **534**, L177 and references therein.
15. P. Ullio 1999, astro-ph/9904086 and Frascati Physics Series Vol. XXIV, 475, (2002).
16. P. Fleury, Frascati Physics Series Vol. XXIV, 305, (2002).
17. L. Feng *et al.*, *Phys. Rev. D* **63**, 045024 (2001) [astro-ph/0008115].
18. M. Grosse Perdekamp *et al.*, *Nucl. Phys. Proc. Suppl.* **76** (1999) 253.
19. A. L. Kagan and M. Neubert, *Eur. Phys. J.* **C7** (1999) 5 [hep-ph/9805303].
20. AMANDA Collaboration, E. Dalberg *et al.*, HE.5.3.06, 26th ICRC (1999). C. Spiering *et al.*, astro-ph/9906205. NESTOR Collaboration, <http://www.uoa.gr/~nestor>. ANTARES Collaboration, J. R. Hubbard *et al.*, HE.6.3.03 26th ICRC (1999).
21. DAMA Collaboration, R. Bernabei *et al.*, *Phys. Lett.* **B480** (2000) 23.  
CDMS Collaboration, R. W. Schnee *et al.*, *Phys. Rept.* **307** (1998) 283 .  
CRESST Collaboration, M. Bravin *et al.*, *Astropart. Phys.* **12** (1999) 107 [hep-ex/9904005].